Hyperbolic non-Euclidean elastic strips and almost minimal surfaces

Efi Efrati and Eran Sharon
The Racah Institute of Physics, The Hebrew University, Jerusalem IL-91904, Israel

Raz Kupferman
Institute of Mathematics, The Hebrew University, Jerusalem IL-91904, Israel

(Received 2 June 2010; revised manuscript received 14 February 2011; published 13 April 2011)

We study equilibrium configurations of thin and elongated non-Euclidean elastic strips with hyperbolic two-dimensional reference metrics $\bar{a}$ which are invariant along the strip. In the vanishing thickness limit energy minima are obtained by minimizing the integral of the mean curvature squared among all isometric embeddings of $\bar{a}$. For narrow strips these minima are very close to minimal surfaces regardless of the specific form of the metric. We study the properties of these "almost minimal" surfaces and find a rich range of three-dimensional stable configurations. We provide some explicit solutions as well as a framework for the incorporation of additional forces and constraints.

DOI: 10.1103/PhysRevE.83.046602 PACS number(s): 46.25.Cc, 87.10.Pq

I. INTRODUCTION

In many naturally forming systems simple local growth rules result in complex shapes (see, e.g., Sharon *et al.* [1]). Often the complexity of the shapes is due to geometrical constraints, namely the unavailability of configurations that preserve the symmetries of the underlying growth rule. For example, in Ref. [1] a featureless constant growth enhancement along the perimeter of an eggplant leaf results in a wavy pattern, generated in order to accommodate the excess in area.

Unlike standard buckling and crumpling mechanisms (of stress-free bodies) that are associated with external forces or confinement, in the case described above the confinement is imposed by the ambient Euclidean space which precludes the existence of stress-free configurations. We refer to the latter case as shaping through geometric frustration.

In the mechanical context geometric frustration is manifested as residual stress (the presence of stress in the absence of external forces). The identifying characteristic of residually stressed bodies is that their configuration changes significantly if their integrity is compromised. For example, Vandivier and Goriely [2] showed by dissecting a residually stressed rhubarb stalk how the various peels undergo a significant change in length once disconnected one from the other. Conversely, if the dissection of a growing tissue causes a change in shape of its constituents, then the mechanical description of the tissue must take into account residual stress.

A hyperelastic theory that connects residual stress to geometric frustration has been available for several decades (see, for example, Wang [3] and Kröner [4]). For homogeneous and isotropic (amorphous) materials the only local property characterizing the body is a reference metric (rest distances between material elements). The energy density within a body of a given configuration is a function of the metric discrepancy between the reference metric and the actual metric associated with the configuration. Geometric frustration occurs when the reference metric cannot be embedded in the ambient three-dimensional Euclidean space (i.e., the reference metric is nonflat).

Thin elastic bodies are often described by reduced 2D theories [5] in which the thin body is modeled as a two-dimensional surface embedded in three-dimensional space. Such a surface is uniquely determined (modulo rigid motion) by its two fundamental forms which must satisfy compatibility conditions. The prescription of a three-dimensional reference metric on a thin body is modeled by the prescription of reference first and second fundamental forms. Geometric frustration corresponds to incompatible first and second fundamental forms [6].

A subclass of incompatible thin bodies, named non-Euclidean plates, corresponds to the case where the reference second fundamental form vanishes identically, but the reference first fundamental form (the two-dimensional metric) is nonflat, that is, has a nonvanishing Gaussian curvature. In such bodies the only shaping mechanism is the two-dimensional reference metric [7]. The elastic energy of such plates can be decomposed into a stretching term which measures strains along the midsurface and a bending term. The stretching vanishes for isometric embeddings of the two-dimensional reference metric, whereas the bending term vanishes only for planar configurations.

Non-Euclidean plates can be viewed as composed of identical surfaces stacked one on top of the other, each of the surfaces being nonplanar. Whenever a thin sheet bends, the outer layer (with respect to the curvature of the sheet) elongates compared to the inner layer. It is the invariance of the geometry of the layers that renders these sheets "plate-like", such that they assume a vanishing bending energy only for flat configurations. For further discussion about the properties of non-Euclidean plates and naturally occurring examples the reader is referred to the review [8].

Finding the elastic equilibrium configuration of extremely thin non-Euclidean plates amounts to finding the bending-minimizing isometry of their two-dimensional reference metric [9,10]. In general, finding a bending-minimizing isometry of a given two-dimensional metric is a formidable task which can be solved explicitly only in very particular cases. Naively, one would attempt to minimize the bending energy density locally, however, the compatibility conditions preclude the existence of such solutions [6]. In the present work we identify one particular scenario in which local bending minimization

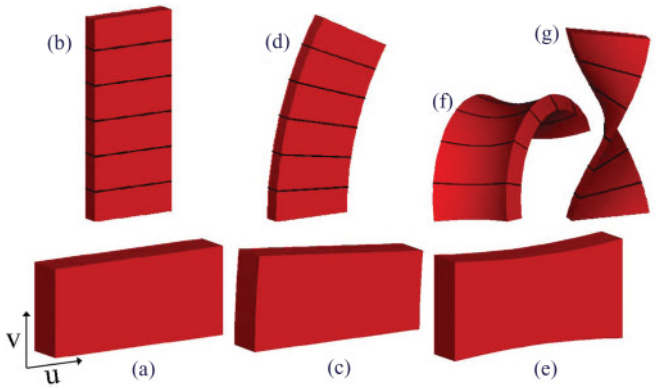

FIG. 1. (Color online) An illustration of Euclidean and non-Euclidean strips. Three types of unit cells are depicted, and above each such unit cell we display strips obtained by stacking multiple copies of them one on top of the other. (a) A rectangular block: the side length along the v direction is constant. (b) When multiple blocks are stacked one on top of the other along the v direction a straight thin and narrow strip is obtained. (c) A block whose length along the v direction varies linearly with the u coordinate. (d) When multiple blocks are stacked the resulting strip remains planar, yet curves in the plane to accommodate the length variation. (e) A block displaying a nonlinear length variation. When such blocks are stacked along the v direction the resulting strip must curve out of plane in order to accommodate the nonlinear length variation. There are many different configurations compatible with the prescribed lengths. Two such configurations are depicted: (f) a catenoid-like configuration and (g) a helicoidal configuration. In the limit of vanishing unit cell length, the length variation within the unit cell maps onto a metric for the strip. A nonlinear length variation along the v direction yields a non-Euclidean metric.

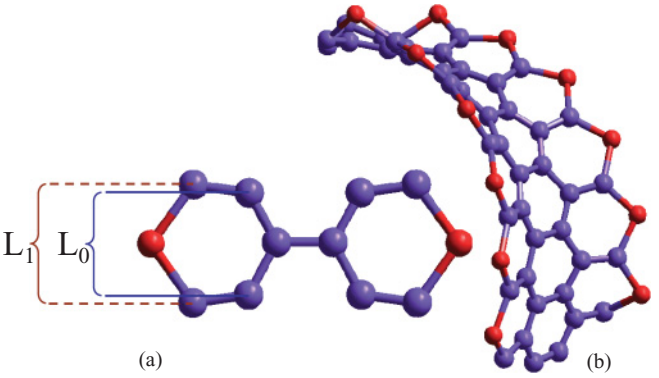

FIG. 2. (Color online) An illustration of a nanometric non-Euclidean strip. Silicon doped carbon nanoribbon. (a) A single carbon base unit cell in which the right-most and left-most atoms were replaced by silicon atoms. The silicon-carbon bond length (L_1) is roughly 15% longer than the carbon-carbon bond length (L_0). When a single unit cell is considered, its equilibrium configuration lays in the plane. (b) When six such unit blocks are connected, the resulting ribbon will bend out of plane to accommodate the length variation across its width, similarly to the strip in Fig. 1(f). The length scale of the Gaussian curvature associated with the silicon doping-induced elongation is of the order of the width of the strip. Therefore, while the strip depicted in (b) is a non-Euclidean plate, it cannot be considered narrow. The figures above are only illustrations; for further details see [11].

can approximate the sought isometry: narrow strips, that is, plates in which an additional dimension is relatively small.

In the schematic illustration in Fig. 1, Euclidean and non-Euclidean strips are composed of "unit cells". The length variation of the unit cells effectively endows the sheets with a metric. Since a unit cell is flat and contains no structure across it thickness, the resulting strip will have no tendency to bend, hence will have a vanishing second fundamental form. While no strain needs to be introduced to stack the compatible cells [1(a), 1(c)], there is a need to deform at least one of of the blocks in the incompatible case [1(e)].

The unit cells in Fig. 1 can be interpreted as arbitrary sections of a continuous growing tissue, such as that of a plant leaf. For example, inhomogenous differential growth can transform the unit cell depicted in Fig. 1(a) into the unit cell depicted in Fig. 1(e). The corresponding equilibrium configuration appearing in Fig. 1(b) will transform into a buckled configuration similar to that in Fig. 1(f). In this sketch, the unit cells are discrete realizations of a spatially varying metric. For examples of such strips, the reader is referred to [12,13] where the nonuniform growth of an algae blade (as well as the nonuniform irreversible deformation of a thin sheet) is shown to result in configurations similar to those in Figs. 1(f) and 1(g). The growth (or irreversible deformation) in these systems induces the non-Euclidean metric. As the growth (or irreversible deformation) profile does not significantly vary across the thickness, no reference curvatures are prescribed and the resulting strips are plate-like.

An alternative interpretation of the unit cells depicted in Fig. 1 is as molecular building blocks. These building blocks can be composed of large molecules that self-assemble to form ribbon-like macromolecular structures of a micron scale [14], or contain just a few atoms and form structures of nanometric scale (as described in Fig. 2). In both cases, whenever the building blocks are symmetric (about their midsurface), the resulting macromolecule possess no reference curvature. While nanometric structures cannot be considered narrow, macromolecules of micrometric dimensions [14], as well as elongated leaves [12] and some algae blades [13], exhibit large aspect ratios in all three dimensions, that is, they are both thin and narrow. Thus, studying equilibrium configurations of hyperbolic non-Euclidean strips is important for our understanding of both macroscale and microscale chemical and biological structures.

Finding a bending energy minimizing isometry of a narrow and long *flat* strip has been addressed more than 80 years ago by Sadowsky [15]. Mansfield [16] accounted for the finite width perturbatively, and more recently Starostin and van der Heijden [17] carried out an exact analysis of wide strips to find the bending minimizing conformation of a developable möbius strip (which is topologically constrained). Recently Marder and Papanicolaou [18] considered flat strips with linear metric gradients, and showed that under suitable boundary conditions elastic equilibria assume helical shapes. While for a flat strip the unconstrained problem yields only a trivial solution, when considering a hyperbolic metric even very narrow unconstrained strips give rise to nontrivial bending minimizing embeddings.

Here we study in detail non-Euclidean strips whose intrinsic geometry is translationally invariant along their longitudinal direction. We construct approximate elastic equilibria which we term "almost minimal", as their mean curvature is uniformly small. These surfaces have, in the general case, a discrete symmetry. The fundamental forms are periodic, however the resulting surfaces are not necessarily closed. We show that in order to characterize these solutions it is sufficient to predict the shape of a single curve along the strip, which we take to be the midcurve. This procedure yields a unique energy minimizer (for an infinite strip) whose bending energy scales like w^5.

As long as the width of the strip is immaterial to the configuration, we can identify all the properties of the surface with the shape of the midcurve and express the bending energy of the strip as a functional of the configuration of the midcurve. The latter is fully determined by the local curvature κ and torsion τ. Such an elastic energy depending only on κ and τ and not on the twist field is typical for anisotropic rods having an infinite bending stiffness in one direction. As a result of the anisotropy the relative orientation of the material frame of the rod and the Serret-Frenet frame of its centerline is prescribed [19]. While the rod-like energy density given by the square of (C5) may seem artificial in the context of rods, it arises naturally in the context of thin narrow non-Euclidean strips.

The bending energy minimizer, whose energy is of order w^5, resides in a shallow "energy well" comprised of a continuum of configurations with energies of order w^3. This implies the existence of a "soft" deformation mode along which the energy gradient is very weak. By characterizing this family of low-energy configurations, we are able to include in our treatment unconstrained strips of finite length as well as additional boundary conditions and external potentials.

II. NON-EUCLIDEAN PLATES

The intrinsic geometry of a residually stressed amorphous body is characterized by a three-dimensional reference metric $\bar{g}$ that cannot be immersed isometrically in the ambient three-dimensional Euclidean space (e.g., [20] and references therein). Thus, every immersion (i.e., physical configuration) necessarily involves a metric discrepancy—a strain—with respect to the reference metric $\bar{g}$, and the equilibrium is postulated to be the configuration that minimizes the elastic energy associated with this metric discrepancy. In Ref. [6] the elastic energy was taken to be a mean square difference between the actual metric and the reference metric, but other energy functions can be considered readily within this formalism.

A reduced two-dimensional theory was derived (using a formal asymptotic expansion) for the case where the elastic body is thin, that is, when the (finite) thickness t of the body is smaller than all other length scales [21]. The reduced model was given the name of either *non-Euclidean plate* or *non-Euclidean shell*, depending on whether the reference metric varies along the thin dimension (shells) or not (plates). A non-Euclidean plate is modeled as a surface immersed in $\mathbb{R}^3$, that is, as a mapping $\boldsymbol{f} : \mathcal{S} \to \mathbb{R}^3$, where $\mathcal{S} \subset \mathbb{R}^2$ is the domain of parametrization; points in $\mathcal{S}$ are denoted by $x = (x_1, x_2)$. Recall that the first and second fundamental forms of a surface in $\mathbb{R}^3$ are given by (e.g., [22])

$$a_{\alpha\beta} = \partial_\alpha \boldsymbol{f} \cdot \partial_\beta \boldsymbol{f} \quad \text{and} \quad b_{\alpha\beta} = \partial_\alpha \partial_\beta \boldsymbol{f} \cdot \boldsymbol{\mathcal{N}}, \tag{1}$$

where $\partial_\alpha = \partial/\partial x^\alpha$ and $\boldsymbol{\mathcal{N}}$ is the unit vector normal to the surface; here and below we use Greek characters to denote the indices 1,2. (The surface is assumed to be orientable, not, for example, a Möbius strip, in which case a continuous unit normal can be defined unambiguously.) The (dimensionless) elastic energy per unit thickness associated with a non-Euclidean plate is

$$\mathcal{E}[\boldsymbol{f}] = \mathcal{E}_S[\boldsymbol{f}] + t^2\, \mathcal{E}_B[\boldsymbol{f}], \tag{2}$$

where

$$\mathcal{E}_S = \int_S \mathcal{A}^{\alpha\beta\gamma\delta}(a_{\alpha\beta} - \bar{a}_{\alpha\beta})(a_{\gamma\delta} - \bar{a}_{\gamma\delta})\, dS$$

and

$$\mathcal{E}_B = \frac{1}{3}\int_S \mathcal{A}^{\alpha\beta\gamma\delta} b_{\alpha\beta} b_{\gamma\delta}\, dS$$

are the stretching and bending contents, respectively, $\bar{a}_{\alpha\beta}$ is a two-dimensional reference metric, $dS = \sqrt{|\bar{a}|}dx_1 dx_2$ is the surface element, and

$$\mathcal{A}^{\alpha\beta\gamma\delta} = \frac{\nu}{1-\nu}\bar{a}^{\alpha\beta}\bar{a}^{\gamma\delta} + \frac{1}{2}(\bar{a}^{\alpha\gamma}\bar{a}^{\beta\delta} + \bar{a}^{\alpha\delta}\bar{a}^{\beta\gamma})$$

is the elastic tensor. Here ν is the Poisson ratio and $\bar{a}^{\alpha\beta}$ is the tensor reciprocal to $\bar{a}_{\alpha\beta}$. We use Einstein's summation rule, whereby repeated indices imply a summation.

The two-dimensional reference metric $\bar{a}$ is induced by a three-dimensional reference metric $\bar{g}$, which does not vary across the thin dimension ($\bar{a}$ is the projection of $\bar{g}$ onto the manifold tangent to the midsurface). The nonimmersibility of a three-dimensional plate metric $\bar{g}$ reflects in the two-dimensional metric $\bar{a}$ being nonflat, that is, having a nonzero Gaussian curvature [6]. In such case, the energy is necessarily positive as the stretching term is zero if and only if $a_{\alpha\beta} = \bar{a}_{\alpha\beta}$, whereas the bending term is zero if and only if the surface is flat, namely $b_{\alpha\beta} = 0$. Since the Gaussian curvature is an isometric invariant this cannot occur if $\bar{a}$ is nonflat [23].

The first and second fundamental forms of a surface (1) are not independent. They are constrained by a set of algebraic-differential equations, the Gauss–Mainardi–Peterson–Codazzi (GMPC) equations,

$$\begin{aligned} \partial_2 b_{11} - \partial_1 b_{12} &= b_{11}\Gamma^1_{12} + b_{12}\left(\Gamma^2_{12} - \Gamma^1_{11}\right) - b_{22}\Gamma^2_{11}, \\ \partial_2 b_{12} - \partial_1 b_{22} &= b_{11}\Gamma^1_{22} + b_{12}\left(\Gamma^2_{22} - \Gamma^1_{12}\right) - b_{22}\Gamma^2_{12}, \\ b_{11}b_{22} - b^2_{12} &= K\left(a_{11}a_{22} - a^2_{12}\right), \end{aligned} \tag{3}$$

where $\Gamma^\alpha_{\beta\gamma}$ are the Chistoffel symbols associated with the Riemannian connection,

$$\Gamma^\alpha_{\beta\gamma} = \tfrac{1}{2}a^{\alpha\eta}(\partial_\beta a_{\eta\gamma} + \partial_\gamma a_{\eta\beta} - \partial_\eta a_{\beta\gamma}) \tag{4}$$

and K is the Gaussian curvature, which by Gauss' theorem only depends on the first fundamental form and its derivatives. The two-dimensional elastic problem thus consists of finding the immersion $\boldsymbol{f}$ that minimizes the elastic energy (2). Equivalently, it consists of finding first and second fundamental forms a, b that minimize the energy (2) under the constraints

of the GMPC equations (3). It should be noted that in the latter case the space of admissible metrics consists of continuous, nonsingular metrics, which ensures that the immersion is orientation preserving. This local condition does not prevent the surface from intersecting itself in the large. Models that take into account nonlocal interactions are notoriously harder to work with. On the other hand, if the optimal immersion turns out to be an embedding, then it is automatically also the optimal embedding.

The thickness of the plate t plays a fundamental role as a parameter that determines the relative weight of the stretching and the bending. Very thin plates tend to minimize the stretching, that is, to be close to isometric immersions of the reference metric $\bar{a}_{\alpha\beta}$, whereas thicker plates tend to minimize the bending, that is, assume flat, or nearly flat configurations. Analyses of the thin-plate limit were presented in [9,10] with the following outcomes.

(1) Assuming that the metric $\bar{a}$ admits an isometric immersion with finite bending content, any sequence of (approximate) minimizers converges as $t \to 0$ to an isometric immersion of $\bar{a}$ that minimizes the bending content. (More precisely, there is a subsequence that converges to a minimizer of the bending content; if such a minimizer is unique then the whole sequence converges.). This result was proved in [10] using Γ-convergence techniques starting from a model of three-dimensional incompatible elasticity. It is not hard to see that this implies convergence to the same limit if one departs from the two-dimensional model of non-Euclidean plates.

(2) Under the same assumptions the deviation from the vanishing thickness limit (for finite but small thickness) is localized in a narrow layer at the boundary of the domain. The width of this boundary layer scales like $(t/\kappa_{\|})^{1/2}$, where $\kappa_{\|}$ is the normal curvature of the surface along the boundary (in the unperturbed bending-minimizing isometry).

For an isometric immersion, that is, $a = \bar{a}$, the bending content is equal to

$$\mathcal{E}_B = \frac{1}{3}\int_S \left[\frac{\nu}{1-\nu}(k_1+k_2)^2 + k_1^2 + k_2^2\right] dS = \frac{1}{3}\int_S \left(\frac{4H^2}{1-\nu} - 2K\right) dS, \tag{5}$$

where k_1 and k_2 are the principal curvatures and $H = \frac{1}{2}\mathrm{tr}(a^{-1}b) = \frac{1}{2}(k_1+k_2)$ is the mean curvature. Since K is a metric invariant, the minimum bending is obtained by minimizing the so-called Willmore energy ([24], p. 106)

$$\mathcal{E}_W = \int_S H^2\, dS \tag{6}$$

with respect to all isometric immersions of the given metric $\bar{a}$.

III. HYPERBOLIC SURFACES

Considering the second fundamental form b as the unknown and the first fundamental form $a = \bar{a}$ as given, the type of the GMPC equations (3) depends on the type of the surface. Elliptic surfaces $K > 0$ give rise to an elliptic system of equations, whereas hyperbolic surfaces $K < 0$ give rise to a hyperbolic system of equations. We focus on the second case. For hyperbolic surfaces a useful change of variables reduces the system of three algebraic-differential equations (3) into a system of two quasilinear differential equations which can be attributed a natural geometric interpretation. Define

$$k = (-K)^{1/2} \quad \text{and} \quad q = |a|^{1/2},$$

where $|a| = \det(a)$. A hyperbolic surface has at every point a pair of asymptotic directions along which the normal curvature vanishes. The tangents of the angles that the asymptotic curves form with respect to the x_1 direction, denoted by r and s, are given by

$$r = \frac{-b_{12} - qk}{b_{22}} \quad \text{and} \quad s = \frac{-b_{12} + qk}{b_{22}}. \tag{7}$$

The inverse transformation from r,s to the second fundamental form is

$$b_{11} = \frac{2rsqk}{s-r}, \quad b_{12} = -\frac{(r+s)qk}{s-r}, \quad \text{and} \quad b_{22} = \frac{2qk}{s-r}. \tag{8}$$

As derived by Rozhdestvenskii [25] and Shikin and Poznyak [26], substituting (8) into the GMPC equations (3) yields

$$\begin{aligned} \partial_1 r + s\,\partial_2 r &= F(r,s,x), \\ \partial_1 s + r\,\partial_2 s &= F(s,r,x), \end{aligned} \tag{9}$$

where

$$F(r,s,x) = A_0 + A_1 r + A_2 s + A_3 r^2 + A_4 rs + A_5 r^2 s,$$

and the coefficients $A_i = A_i(x)$ are metric invariants

$$\begin{aligned} A_0 &= -\Gamma^2_{11}, \quad A_1 = -\Gamma^2_{12} + \Gamma^1_{11} + \frac{\partial_1 k}{2k}, \\ A_2 &= -\Gamma^2_{12} - \frac{\partial_1 k}{2k}, \quad A_3 = \Gamma^1_{12} + \frac{\partial_2 k}{2k}, \\ A_4 &= \Gamma^1_{12} - \Gamma^2_{22} - \frac{\partial_2 k}{2k}, \quad A_5 = \Gamma^1_{22}. \end{aligned} \tag{10}$$

The system (9), viewed as a differential system for r,s with $a_{\alpha\beta}$ given, has a number of remarkable properties.

(1) It is symmetric with respect to the transformation $r \leftrightarrow s$, which simply reflects the fact that there is nothing that distinguishes one family of asymptotic curves from the other.

(2) The variables r and s are Riemann invariants, namely their value along characteristic curves is only affected by lower order terms (e.g., [27] p. 593). Moreover, r is the slope (or speed) of the characteristic curve that carries s and vice versa. That is, $(\partial_1 + r\partial_2)s$ is the rate-of-change of the slope s of an asymptotic curve along the other asymptotic curve whose slope is r.

(3) The system (9) does not exclude situations where $r = s$, yet it loses then its geometrical meaning. When $r = s$ not only do the two characteristic curves locally coincide, but also the transformation (8) inverse to (7) shows that the second fundamental form diverges.

(4) In the context of a hyperbolic system we may view x_1 as a "time coordinate" and x_2 as a "space coordinate". This distinction is of course artificial, and sensible only if "initial data" are provided along a constant-x_1 parametric curve (which may be the case, for example, if the shape of the surface is imposed along a boundary).

(5) While as a differential system (9) requires r and s to be real valued, situations where $r,s = \pm\infty$ make perfect geometric sense, as they only mean that the asymptotic curves are tangent to constant-x_1 parametric curves. The question of how to cope with the tangency of the initial data curve and characteristics is briefly addressed in the Appendix A, but to a large extent remains open.

(6) The low-order source terms on the right-hand side, $F(r,s,x)$ and $F(s,r,x)$, are cubic polynomials, and therefore may lead to finite-"time" blowup. This blowup is sometimes related to the "finite horizon" of hyperbolic surfaces which occurs when $r = s$ or $1/r = 1/s = 0$.

The knowledge of r and s, along with the first fundamental form, is equivalent to the knowledge of the two fundamental forms and by the fundamental theorem of surface geometry uniquely determines the surface up to rigid transformations. The fact that the two variables r,s (given the first fundamental form) embody the same information as the three variables b_{11},b_{12},b_{22} results from Gauss's *theorema egregium*, whereby the Gaussian curvature is a metric invariant. In particular, the mean curvature H can be expressed in terms of the variables r,s,

$$H = \frac{1}{2}a^{\alpha\beta}b_{\beta\alpha} = \frac{k}{q}\frac{a_{11} + a_{12}(r+s) + a_{22}rs}{s-r}. \tag{11}$$

IV. NON-EUCLIDEAN STRIPS

We now turn our attention to a subclass of non-Euclidean plates, which we name *non-Euclidean strips*. The domain of parametrization is assumed to be of the form

$$\mathcal{S} = [-w/2, w/2] \times [0, L], \tag{12}$$

where w and L stand for "width" and "length", with a two-dimensional reference metric (in semigeodesic form) that is independent of x_2,

$$\bar{a}_{\alpha\beta} = \begin{pmatrix} 1 & 0 \\ 0 & \varphi^2(x_1) \end{pmatrix}, \tag{13}$$

that is, the intrinsic geometry of the body is invariant along the strip. Since $\bar{a}_{11} = 1$ it follows that this surface is a strip of constant width w. Our working hypothesis is that $t \ll w \ll L$, that is, we are in a regime of *thin and narrow* strips. Without loss of generality we may also assume that $\varphi(0) = 1$, that is, the $x_1 = 0$ parametric curve (the midcurve) has arclength parametrization, and that the Gaussian curvature along the midcurve has absolute value $|K| = 1$ (which amounts to a choice of unit length scale).

Example. As a canonical example consider the case where the Gaussian curvature is constant and equal to $K = -1$, that is, $k = (-K)^{1/2} = 1$. The family of functions φ that corresponds to this choice is

$$\varphi(x_1) = \cosh x_1 - \kappa_g \sinh x_1, \tag{14}$$

where κ_g is the geodesic curvature of the midcurve. The particular choice $\kappa_g = 0$ corresponds to the case where midcurve is a geodesic, in which case the geometry of the strip is symmetric with respect to reflections about the midcurve.

We require the width w of the strip to be large not only compared to its thickness but also compared to the width of the bending-dominated boundary layer. Assuming that the magnitudes of the two principal curvatures are comparable, $|k_1| \sim |k_2| \sim k = |K|^{1/2}$, then the width of the boundary layer is of order $t^{1/2}k^{-1/2}$. Thus, our scaling assumption amounts to

$$t \ll t^{1/2}|K|^{-1/4} \ll w \ll K^{-1/2} \ll L. \tag{15}$$

Under these scaling assumptions we may consider the surface as an isometric immersion of the reference metric $a = \bar{a}$, hence from now on we no longer distinguish between the reference metric $\bar{a}$ and the actual metric a; finding a configuration amounts to solving (9).

The special form (13) of the reference metric slightly simplifies the system (9). The Christoffel symbols (4) are given by

$$\Gamma^1 = \begin{pmatrix} 0 & 0 \\ 0 & -\varphi\varphi' \end{pmatrix} \quad \text{and} \quad \Gamma^2 = \begin{pmatrix} 0 & \varphi'/\varphi \\ \varphi'/\varphi & 0 \end{pmatrix}, \tag{16}$$

whereas the Gaussian curvature is given by

$$-K = k^2 = \frac{\varphi''}{\varphi},$$

with primes denoting derivatives with respect to x_1. We also note that the geodesic curvature of the midcurve (which is an isometric invariant) is given by

$$\kappa_g = |a(0)|^{1/2}\Gamma^1_{22}(0) = -\varphi'(0).$$

Substituting the metric (13) into the coefficients $A_i(x)$ given by (10), the hyperbolic system (9) reduces to

$$\begin{aligned} \partial_1 r + s\,\partial_2 r &= A_1 r + A_2 s + A_5 r^2 s, \\ \partial_1 s + r\,\partial_2 s &= A_1 s + A_2 r + A_5 s^2 r, \end{aligned} \tag{17}$$

where

$$A_1 = -\frac{\varphi'}{\varphi} + \frac{k'}{2k}, \quad A_2 = -\frac{\varphi'}{\varphi} - \frac{k'}{2k}, \quad \text{and} \quad A_5 = -\varphi\varphi'. \tag{18}$$

Finally, the mean curvature (11) reduces to

$$H = \frac{k(1+\varphi^2 rs)}{\varphi(s-r)},$$

so that the Willmore energy (6) (which is proportional to the total energy in the case of an isometry) is

$$\mathcal{E}_W[r,s] = \int_0^L \int_{-w/2}^{w/2} \frac{k^2(1+\varphi^2 rs)^2}{\varphi(r-s)^2}\, dx_1 dx_2. \tag{19}$$

The theorem in [10] (adapted to the two-dimensional setting) states that as $t \to 0$ the surface approaches an isometric immersion, with (r,s) being the solution of the hyperbolic system (17) that minimizes the Willmore energy (19). This alternative point of view, even though formulated using variables that are natural when dealing with hyperbolic surfaces, retains the main difficulty of the original problem. The variational functions r and s are not independent, and the Euler-Lagrange equations arising from this constrained optimization problem form a nonlinear second-order system. In the next section we present an approximation method for solving this constrained optimization problem.

V. ALMOST-MINIMAL STRIPS

Minimal surfaces are surfaces whose mean curvature is identically zero. Such surfaces appear naturally in problems governed by surface tension, as they minimize the area of the surface given the shape of its boundary, hence their name (e.g., Struik [22], p. 182). Since minimal surfaces trivially minimize the Willmore energy (6), then if we could find an isometric immersion of the reference metric $\bar{a}$ that is also a minimal surface, it would automatically be the solution to our problem, that is, the $t \to 0$ limiting configuration. Thus, one may be tempted to look for isometric immersions that are minimal surfaces. It is well known, however, that not every hyperbolic metric admits immersions that are minimal surfaces. A hyperbolic metric $a_{\alpha\beta}$ can be immersed as a minimal surface if and only if it satisfies the condition (due to Ricci) that $k\, a_{\alpha\beta}$ is a flat metric (of vanishing Gaussian curvature), where as above $k = (-K)^{1/2}$ [28]. When applied to a metric of the form (13), the Ricci condition takes the explicit form

$$3\varphi''^3 - \varphi\varphi''''^2 + \varphi'\varphi''\varphi'''' + \varphi\varphi''\varphi'''' = 0. \tag{20}$$

Thus, energy minimizing isometries are minimal surfaces only in the case of a strip geometry with $\varphi(x_1)$ satisfying (20).

The fourth-order ordinary differential equation (20) defines a family of metrics parametrized by four constants which could be taken to be the values of φ and its first three derivative at $x_1 = 0$. Given a hyperbolic metric of the form (13) with prescribed $\varphi(x_1)$, there exists a solution φ_M of (20) that matches φ and its first three derivatives at $x_1 = 0$. The difference between φ and φ_M satisfies the uniform bound

$$\varphi - \varphi_M = O(w^4).$$

Denote by r_M and s_M solutions of (17) with φ replaced by φ_M that give rise to minimal surfaces. Since the right-hand side of (17) depends explicitly on the third derivative of φ (via k'), a straightforward estimate shows that a solution r,s, of (17) with initial conditions $r(0) = r_M(0)$ and $s(0) = s_M(0)$ satisfies

$$r - r_M = O(w^2) \quad \text{and} \quad s - s_M = O(w^2),$$

which in turn implies a Willmore energy of order w^5. The conclusion of these considerations is that given a narrow hyperbolic strip we may find an immersion that approximates a minimal surface and whose Willmore energy scales like the fifth power of the strip's width. We call such immersions *almost minimal*.

The existence of minimal solutions r_M and s_M for metrics φ_M satisfying Ricci's condition is shown explicitly in the next subsection. These solutions involve a divergence of r_M and s_M at a periodic array of points. While not problematic by its own, this divergence poses a problem when considering perturbations. We address this delicate issue in Appendix A.

To find such an almost-minimal solution, we formally expand the Riemann invariants r,s in powers of x_1,

$$\begin{aligned} r(x) &= r_0(x_2) + r_1(x_2)\, x_1 + O\left(x_1^2\right), \\ s(x) &= s_0(x_2) + s_1(x_2)\, x_1 + O\left(x_1^2\right), \end{aligned} \tag{21}$$

which substituted into (17) yields a hierarchy of ordinary differential systems, the first of which being

$$\begin{aligned} r_1 &= -s_0 r_0' + A_1(0) r_0 + A_2(0) s_0 + A_5(0) r_0^2 s_0, \\ s_1 &= -r_0 s_0' + A_1(0) s_0 + A_2(0) r_0 + A_5(0) s_0^2 r_0, \end{aligned} \tag{22}$$

where

$$A_1(0) = \kappa_g + \frac{k'}{2}, \quad A_2(0) = \kappa_g - \frac{k'}{2}, \quad A_5(0) = \kappa_g,$$

and the right-hand sides are evaluated at $x_1 = 0$.

We seek to eliminate as many terms as possible in the expansion of the Willmore energy in powers of the width w. The above considerations imply we can achieve $H = O(x_1^2)$. Eliminating the zeroth and first-order terms

$$H(x_2,0) = 0 \quad \text{and} \quad \partial_1 H(x_2,0) = 0,$$

we need the following relations to hold:

$$r_0 s_0 = -1 \quad \text{and} \quad r_1 s_0 + s_1 r_0 = -2\kappa_g.$$

Substituting these two relations into (22) we obtain

$$r_0' = \frac{\beta}{2}\left(1 + r_0^2\right), \tag{23}$$

where $\beta = 2A_2(0) = 2\kappa_g - k'$. Solving (23),

$$r_0 = \tan\left(\frac{\beta}{2} x_2 + \theta\right) \quad \text{and} \quad s_0 = -\cot\left(\frac{\beta}{2} x_2 + \theta\right).$$

The phase θ is a constant of integration, which generates a one-dimensional family of minimal embeddings. For $\beta \neq 0$ variations in θ correspond to a "sliding mode" along the strip and can be ignored for a sufficiently long strip. For $\beta = 0$ the solutions are translationally invariant (helices) and various choices of θ correspond to distinct solutions (differing in the pitch). The latter case is treated in Sec. VI.

Having found the leading order solutions r_0 and s_0 of (17) (i.e., r and s on the midcurve), we should in principle proceed to solve the hierarchy of equations term-by-term. As argued above, this construction ensures a Willmore energy of order w^5.

The second fundamental form along the midcurve is obtained through the inverse transformation (8):

$$\begin{aligned} b_{11} &= \frac{2}{s_0 - r_0} = \sin\beta x_2, \\ b_{12} &= -\frac{s_0 + r_0}{s_0 - r_0} = -\cos\beta x_2, \\ b_{22} &= -\frac{2}{s_0 - r_0} = -\sin\beta x_2. \end{aligned}$$

The second fundamental form is periodic, with period $2\pi/\beta$, whereas the first fundamental form is translationally invariant. Since the configuration is determined, up to rigid transformations, by the two fundamental forms it follows that the configuration is a concatenation of geometrically identical segments of length $2\pi/\beta$.

To retrieve the configuration of the midcurve we solve the Gauss-Weingarten equations

$$\frac{\partial}{\partial x_2}\begin{pmatrix}\partial_1 \boldsymbol{f}\\ \partial_2 \boldsymbol{f}\\ \boldsymbol{\mathcal{N}}\end{pmatrix} = \begin{pmatrix}0 & -\kappa_g & b_{12}\\ \kappa_g & 0 & b_{22}\\ -b_{12} & -b_{22} & 0\end{pmatrix}\begin{pmatrix}\partial_1 \boldsymbol{f}\\ \partial_2 \boldsymbol{f}\\ \boldsymbol{\mathcal{N}}\end{pmatrix}$$

which are in fact three sets of decoupled systems, one for each of the three component of $\partial_1 \boldsymbol{f}$, $\partial_2 \boldsymbol{f}$, and $\boldsymbol{\mathcal{N}}$. This system can be solved analytically:

$$\begin{aligned}\partial_1 \boldsymbol{f}(0,x_2) &= -\gamma\ \cos\beta x_2\,(\mathbf{b}\sin\gamma x_2 - \mathbf{c}\cos\gamma x_2)\\ &\quad - \sin\beta x_2 \frac{\mathbf{a} + (1-\gamma^2)(\mathbf{b}\ \cos\gamma x_2 + \mathbf{c}\ \sin\gamma x_2)}{(\beta-\kappa_g)},\\ \partial_2 \boldsymbol{f}(0,x_2) &= -\gamma\ \sin\beta x_2\,(\mathbf{b}\sin\gamma x_2 - \mathbf{c}\cos\gamma x_2)\\ &\quad + \cos\beta x_2 \frac{\mathbf{a} + (1-\gamma^2)(\mathbf{b}\ \cos\gamma x_2 + \mathbf{c}\ \sin\gamma x_2)}{(\beta-\kappa_g)},\\ \boldsymbol{\mathcal{N}}(0,x_2) &= \mathbf{a} + \mathbf{b}\ \cos\gamma x_2 + \mathbf{c}\ \sin\gamma x_2,\end{aligned} \tag{24}$$

where $\gamma^2 = 1 + (\beta - k_g)^2$. The vectors $\mathbf{a}$, $\mathbf{b}$, and $\mathbf{c}$ are nine constants of integration determined by the initial orientation of the curve which we set to be

$$\begin{aligned}\partial_1 \boldsymbol{f}(0,0) &= (1,0,0),\\ \partial_2 \boldsymbol{f}(0,0) &= (0,1,0),\\ \boldsymbol{\mathcal{N}}(0,0) &= (0,0,1),\end{aligned}$$

yielding

$$\begin{aligned}\mathbf{a} &= \gamma^{-2}(0,\beta-\kappa_g,\gamma^2-1),\\ \mathbf{b} &= \gamma^{-2}(0,\kappa_g-\beta,1),\\ \mathbf{c} &= \gamma^{-1}(1,0,0).\end{aligned} \tag{25}$$

Having an analytical expression for the vector $\partial_2 \boldsymbol{f}(0,x_2)$, the midcurve $\boldsymbol{f}(0,x_2)$ is retrieved by one more integration with respect to x_2, which can also be performed analytically, with suitable initial conditions for $\boldsymbol{f}(0,0)$ (see Appendix B). In Fig. 3 we demonstrate how $\boldsymbol{f}(0,x_2)$ and $\partial_1 \boldsymbol{f}(0,x_2)$ capture most of the morphological traits of a narrow strip.

Example. Consider once again the metric

$$\varphi(x_1) = \cosh x_1 - \kappa_g\ \sinh x_1.$$

This corresponds to the choice $k' = 0$ which leaves us with a single parameter κ_g (the fact that this metric has a constant Gaussian curvature is immaterial here). In Fig. 4 we show the shape of the midcurve for values of κ_g of 0.1, 0.4, 0.7, and 1.0. Each of these curves is a concatenation of identical segments of length $2\pi/\beta$; each such segment is plotted in a different color.

Comments.

(1) As explained above, the midcurve is a concatenation of curves of length $2\pi/\beta$ that are geometrically identical. Yet, since each period involves a translation, a rotation, and a twist the concatenated curve may not seem "geometrically" periodic at first glance.

(2) Consider the location of the midcurve $\boldsymbol{f}(0,x_2)$ at the end points of each period, $x_2 = 2\pi n/\beta \equiv t_n$, $n = 0,1,2,\ldots$.

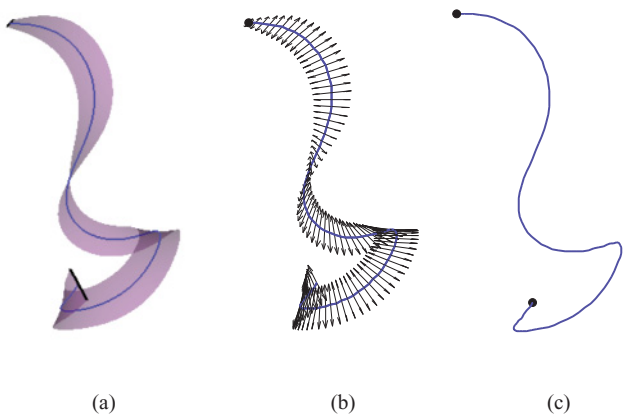

FIG. 3. (Color online) Skeletonization of a strip. An illustration of a single period of a minimal surface. Along the midcurve of the strip $K = -1$ and $k_g = 0.75$. (a) The full surface obtained by the explicit solutions (27) and (28). (b) The "skeleton" of the surface composed from the midcurve (blue) solid curve and tangent vectors $\partial_1 \boldsymbol{f}$ (black) arrows using the explicit formulas (B1) and (24). (c) When studying long and narrow surfaces it is convenient to display only the midcurve and the end points of each period.

A direct integration of $\partial_2 \boldsymbol{f}$ yields, after straightforward algebra,

$$\begin{aligned}\boldsymbol{f}(0,t_n) &= \boldsymbol{f}(0,0) + \frac{\gamma(2\beta-\kappa_g)}{\beta^2-\gamma^2}\\ &\quad \times [\mathbf{c}\,(\cos\gamma t_n - 1) - \mathbf{b}\ \sin\gamma t_n].\end{aligned}$$

Setting $\boldsymbol{f}(0,0) = \gamma(2\beta-\kappa_g)/(\beta^2-\gamma^2)\mathbf{c}$, we obtain at once that all the points $\boldsymbol{f}(0,t_n)$ lie on the plane spanned by the vectors $\mathbf{b}$ and $\mathbf{c}$ along a circle of radius $\gamma(2\beta-\kappa_g)/(\beta^2-\gamma^2)$. Furthermore, considering the tangent vector $\partial_1 \boldsymbol{f}$ at the points $(0,t_n)$ we find that it is parallel to the $\mathbf{b},\mathbf{c}$ plane as well, and perpendicular to the tangent vector $\partial_2 \boldsymbol{f}$ (see Fig. 5).

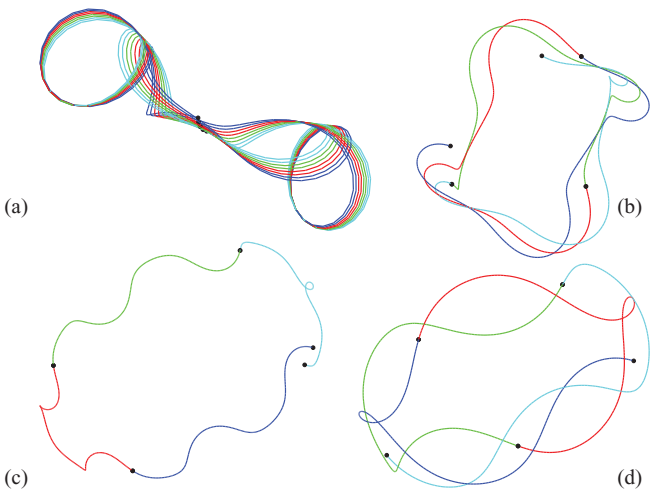

FIG. 4. (Color online) Four periods of the midcurve of four almost minimal surfaces. Along the midcurve of the strips $K = -1$ and the geodesic curvature is (a) $k_g = 0.1$, (b) $k_g = 0.4$, (c) $k_g = 0.7$, and (d) $k_g = 1$. Each period is plotted in a different color and is separated from the next period by a filled (black) circle. The four curves are not to scale.

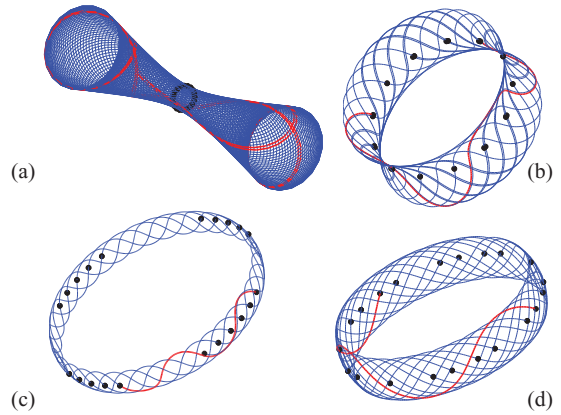

FIG. 5. (Color online) Twenty periods of the midcurve for the same parameter as in Fig. 4. Plotting many periods exemplifies not only that the midcurves are bounded in space, but also that they lie on a surface of revolution. The midcurve is plotted as a solid (blue) line, (black) filled circles locate the periods end points, and the bolded (red) line corresponds to a single period. Note also that all period end points lie on a circle. For graphical reasons the curves are not to scale.

(3) From the previous comments we conclude that $\boldsymbol{f}(0,x_2+2\pi n/\beta)=\mathcal{O}^n\boldsymbol{f}(0,x_2)$, where $\mathcal{O}$ is some proper orthogonal rotation. Moreover, the midcurve lies on a surface of revolution. If $\kappa_g\neq\beta$ it is also bounded.

(4) The midcurve is closed if and only if γ/β is rational.

(5) The case $\beta=0$ deserves special attention, as in this case the phase θ cannot be eliminated by a resetting of the origin of the x_2 coordinate. It follows that there exists a continuous family of distinct solutions, parametrized by the phase θ. This family of solution is further studied in Sec. VI B.

A. Minimal surfaces: Exact solutions

In Figs. 2 and 3 we have only reconstructed the midcurves. Reconstructing the entire surface requires the solution of the hyperbolic system (17). Rather than testing how close are these immersions to being minimal, we may adopt a technically simpler approach. We construct (exact) minimal surfaces and show how close they are to being isometries of the metrics considered above. To do so we solve again the r,s equations (17), assuming this time that the surface is minimal, that is,

$$1+\varphi^2 rs=0,\quad \text{everywhere},$$

however with the metric function φ being yet unknown. Substitution of the minimality condition into (17) gives

$$\begin{aligned}\partial_1 r+s\,\partial_2 r&=\frac{k'}{2k}r+\left(-\frac{\varphi'}{\varphi}-\frac{k'}{2k}\right)s,\\ \partial_1 s+r\,\partial_2 s&=\frac{k'}{2k}s+\left(-\frac{\varphi'}{\varphi}-\frac{k'}{2k}\right)r.\end{aligned}\tag{26}$$

Adding the two equations and using the fact that rs does not depend on x_2 we get

$$\partial_1(r+s)=-\frac{\varphi'}{\varphi}(r+s),$$

from which we deduce that

$$r(x_1,x_2)=\frac{C(x_2)}{\varphi(x_1)}\quad\text{and}\quad s(x_1,x_2)=-\frac{1}{C(x_2)\varphi(x_1)}\tag{27}$$

for some function $C=C(x_2)$. The knowledge of $C(x_2)$ determines the second fundamental form everywhere, thus determines the immersion.

Substitution of (27) into (26) gives

$$\frac{C'}{C^2+1}=-\left(\frac{\varphi'}{\varphi}+\frac{k'}{2k}\right)\varphi.$$

Since the left-hand side only depends on x_2 and the right-hand side only depends on x_1, there exists a constant α such that

$$\frac{C'}{C^2+1}=\alpha\quad\text{and}\quad\left(\frac{\varphi'}{\varphi}+\frac{k'}{2k}\right)\varphi=-\alpha,$$

which gives right away the following x_2 dependence,

$$C(x_2)=\tan(\alpha x_2+\theta),\tag{28}$$

where θ is a phase (which we take again to be zero). It remains to solve the equation for φ. Since the Gaussian curvature is given by

$$K=-k^2=-\frac{\varphi''}{\varphi},$$

it follows that

$$\frac{k'}{k}=\frac{1}{2}\left(\frac{\varphi'''}{\varphi''}-\frac{\varphi'}{\varphi}\right),$$

so that

$$3\varphi'\varphi''+\varphi\varphi'''=-4\alpha\varphi''.$$

After two more integrations we obtain the nonlinear first-order equation

$$\varphi\varphi'+4\alpha\varphi=\beta x_1+\gamma.\tag{29}$$

Equation (29), which was derived from a fourth-order equation, involves three integration constants. Given a metric, we choose the four integration constants such that φ matches the given metric to maximal order. For our running example,

$$\varphi(x_1)=\cosh x_1-\kappa_g\,\sinh x_1,$$

we have

$$\varphi(0)=1,\quad \varphi'(0)=-\kappa_g,\quad \varphi''(0)=1,\quad \varphi'''(0)=-\kappa_g,$$

which yields

$$\alpha=\kappa_g,\quad \beta=1-3\kappa_g^2,\quad\text{and}\quad \gamma=3\kappa_g.$$

We then integrate (29) numerically with initial data $\varphi(0)=1$.

We proceed to reconstruct this family of minimal surfaces which depend on the unique parameter κ_g (in general there is a second parameter k' which is zero in this particular example). With $\varphi(x_1)$ given by the solution to (29), $C(x_2)$ given by (28), $r(x_1,x_2)$ and $s(x_1,x_2)$ given by (27), the Christoffel symbols given by (16), and the second fundamental form related to

r,s,φ through (8), we solve the Gauss-Weingarten equations

$$\partial_2 \begin{pmatrix} \partial_1 \boldsymbol{f} \\ \varphi^{-1}\partial_2 \boldsymbol{f} \\ \boldsymbol{\mathcal{N}} \end{pmatrix} = \begin{pmatrix} 0 & \varphi' & b_{12} \\ -\varphi' & 0 & b_{22}/\varphi \\ -b_{12} & -b_{22}/\varphi & 0 \end{pmatrix} \begin{pmatrix} \partial_1 \boldsymbol{f} \\ \varphi^{-1}\partial_2 \boldsymbol{f} \\ \boldsymbol{\mathcal{N}} \end{pmatrix} \tag{30}$$

and

$$\partial_1 \begin{pmatrix} \partial_1 \boldsymbol{f} \\ \varphi^{-1}\partial_2 \boldsymbol{f} \\ \boldsymbol{\mathcal{N}} \end{pmatrix} = \begin{pmatrix} 0 & 0 & b_{11} \\ 0 & 0 & b_{12}/\varphi \\ -b_{11} & -b_{12}/\varphi & 0 \end{pmatrix} \begin{pmatrix} \partial_1 \boldsymbol{f} \\ \varphi^{-1}\partial_2 \boldsymbol{f} \\ \boldsymbol{\mathcal{N}} \end{pmatrix}. \tag{31}$$

These equations are easily integrated numerically; it takes then one more integration to retrieve the configuration $\boldsymbol{f}$.

In Fig. 6 we show four minimal strips for a fixed width $w = 0.2$ and four values of the geodesic curvature $\kappa_g = 0.1$, 0.4, 0.7, and 1.0. The length of the strip is four periods. By construction the midcurves coincide with the curves in Fig. 4. Even though the width of the strip is a fifth of the characteristic length scale (i.e., the strip is not extremely narrow), the metric discrepancy between these minimal surfaces and the almost-minimal surfaces having the pseudospherical metric (14) is of the order of 10^{-4}. This result is consistent with the estimate of $O(w^4)$ coming from the Ricci minimality condition (20). The corresponding discrepancy between an isometric configuration of any given hyperbolic metric and its minimal strip approximation is therefore expected to be hardly discernible.

The strips depicted in Figs. 6(a) and 6(d) show very different solution strategies, which is to be expected as their geodesic curvatures along the midcurve differ by an order of magnitude.

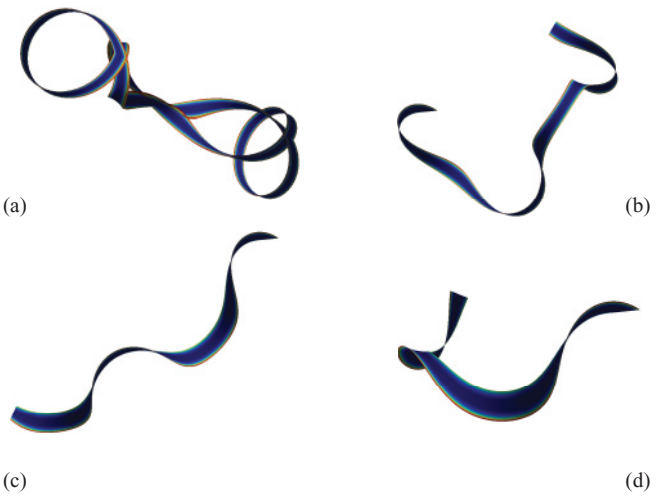

FIG. 6. (Color online) Minimal surfaces. The surfaces were obtained by explicit integration of the Gauss-Weingarten equations (30) and (31). The parameters of the strips are the same as for the previous figures; along the midcurve of the strips $K = -1$ and the geodesic curvature is (a) $k_g = 0.1$, (b) $k_g = 0.4$, (c) $k_g = 0.7$, and (d) $k_g = 1$. Strips colors correspond to longitudinal strain relative to the pseudospherical metric (14), where dark (blue) corresponds to no strain and the lighter (red) colors near the edge correspond to the maximal strain magnitude of 5×10^{-4}.

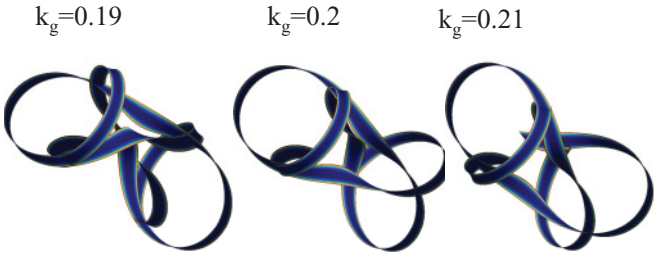

FIG. 7. (Color online) Sensitivity to metric variations. A variation of 1/20 in the geodesic curvature of the midcurve k_g yields very strong morphological changes. All three strips are minimal surfaces calculated as described in (26) and have Gaussian curvature $K = -1$ along their midcurve. One period is plotted for each strip. Colors (same as in Fig. 6) are given for visual purposes.

However, the diversity in solutions does not require, in general, large parametric changes. The high sensitivity to metric variations is exemplified in Fig. 7. One period of three minimal strips whose value of the geodesic curvature along the mid curve differ only by 5 percent show very large morphological differences.

VI. CONSTRAINED MINIMIZATION

In the previous section we showed how to approximate a bending-minimizing isometry of a given metric (i.e., the equilibrium configuration when the strip's thickness is very small) by an almost minimal surface. This approach results in a unique equilibrium configuration whose Willmore energy scales as the fifth power of the width of the strip, namely $\mathcal{E}_W = O(w^5)$. This solution is however not applicable if the setting is supplemented with boundary conditions that are not compatible with the Willmore minimizer, or if other types of constraints are imposed. Specifically, we expect these almost-minimal strips to be relevant only for very long and unconstrained strips. Free strips of finite length, strips of finite length with prescribed edge displacements, and strips whose midcurve is confined to a plane are examples of constrained strips which may not be compatible with the solution presented above. A natural question therefore arises: To what extent can the methodology of the previous section be exploited in these nonideal settings?

When the unique $\mathcal{E}_W = O(w^5)$ solution is not admissible, one expects the equilibrium solution to be selected among the many configurations whose energies have the "second best" scaling in powers of w. By requiring the mean curvature (but not its first derivative) to vanish along the midcurve, it is possible to obtain a very large family of configurations with $\mathcal{E}_W = O(w^3)$. We postulate that these configurations are the natural ones to optimize upon in the presence of nontrivial boundary conditions, or additional admissible constraints. Note, however, that as we treat only isometries of the metric prescribed on the strips, not all constraints or potentials may be treated within the present framework. For example, the prescription of edge displacements may be treated only within a certain range of values that does not necessitate the introduction of in-plane strains. Also, potentials such as surface energy are outside the present scope.

In this section we consider two settings in which minor adaptations of the methodology derived in the previous section enable us to obtain solutions for constrained strips. (A) Unconstrained strips of finite length; the finiteness of the strip imposes boundary conditions at its ends. (B) Configurations constrained to satisfy additional symmetries.

A. Unconstrained strips of finite length

Consider the strip geometry (13) with a finite domain (12). Like in the previous section we expand the Willmore energy in powers of the width w and attempt to eliminate as many terms as possible, eventually minimizing the first term that cannot be eliminated. The terms that scale like the first power of w can be eliminated by setting $H = 0$ along the midcurve. In terms of the formal asymptotic expansion of the Riemann invariants (21), the condition that $H = 0$ along the midcurve implies that

$$1 + r_0 s_0 = 0, \tag{32}$$

thus the next-order contribution to the Willmore energy scales like w^3 and is given by

$$w^3 \int_{-L/2}^{L/2} \frac{(r_0 s_1 + r_1 s_0 - 2\kappa_g r_0 s_0)^2}{(r_0 - s_0)^2}\, dx_2.$$

Substituting r_1 and s_1 given by (22), and using the relation (32) between r_0 and s_0, we obtain an energy that only depends on r_0,

$$w^3 \int_{-L/2}^{L/2} \frac{\left[-r_0' + \frac{\beta}{2}\left(1 + r_0^2\right)\right]^2}{r_0^2}\, dx_2. \tag{33}$$

It is the cancellation of this term that gave rise to the unique solution in the previous section.

Expression (33) can be viewed as a reduced bending energy functional for a thin and narrow strip in which $r_0(x_1)$ is the unique variational function. The corresponding Euler-Lagrange equation yields

$$\frac{r_0'^2 - \left[\frac{\beta}{2}\left(1 + r_0^2\right)\right]^2}{r_0^2} = C, \tag{34}$$

where C is a constant of integration. If the strip is unconstrained, the following zero-torque boundary conditions

$$\frac{\beta}{2}\left(1 + r_0^2\right) - r_0'\Big|_{x_2 = -L/2} = \frac{\beta}{2}\left(1 + r_0^2\right) - r_0'\Big|_{x_2 = L/2} = 0$$

yield $C = 0$, which in turn results in the solution obtained in the previous section, $r_0 = \tan(\frac{\beta}{2}x_2 + \theta)$. In the case of a finite strip we may not set the phase θ arbitrarily to zero, but need to minimize the energy with respect to all possible choices of the phase. As the $O(w^3)$ term vanishes, the selection of the phase θ is governed by the $O(w^5)$ term. It is a simple exercise to show that the latter is minimized by setting $\theta = \pi/2 - \beta L/4$.

B. Translationally invariant configurations

The minimizers of the Willmore energy, with the exception of the case $\beta = 0$, do not preserve the translational symmetry of the metric (they are periodic rather than continuously symmetric). Imposing translational symmetry amounts to setting $r_0' = 0$ and by (34)

$$\frac{-\left[\frac{\beta}{2}\left(1 + r_0^2\right)\right]^2}{r_0^2} = C.$$

The interest in this particular family of solutions is due to two reasons: (i) as argued in the next subsection such a solution is obtained when $\beta = 2\kappa_g - k'(0) = 0$ and (ii) the problem is then analytically solvable since all continuously symmetric embeddings can be written explicitly. As shown in Appendix C the assumption of continuous symmetry gives that all second fundamental forms compatible with the metric $ds^2 = dx_1^2 + \varphi^2(x_1)\, dx_2^2$ form a two-parameter family of solutions,

$$b_{11} = \frac{k}{\kappa}(\tau^2\varphi^{-2} - \kappa^2\varphi^2)\eta, \quad b_{12} = -\frac{\tau k}{\kappa\varphi}, \quad b_{22} = \frac{k}{\kappa\eta},$$

where $\eta = \eta(x_1)$ is given by

$$\eta = [\kappa^2\varphi^2 + \tau^2(\varphi^2 - 1) - \varphi^2\varphi'^2]^{-1/2}.$$

The two parameters are κ and τ which we identify as the (constant) curvature and torsion of the midcurve. No assumptions are made about φ other than inducing a negative Gaussian curvature. Note that the above solution may exhibit a finite horizon in the form of a diverging curvature. Such divergence occur if there exists a point where $\eta \to \infty$ or $\kappa^2 + \tau^2 - \tau^2\varphi^{-2} = \varphi'^2$; whether this happens or not depends on the metric.

To minimize the Willmore energy with respect to the free parameters κ and τ, we set $H = 0$ along the midcurve which corresponds to setting $\kappa^2 + \tau^2 = 1 + \kappa_g^2$. The remaining freedom in the choice of, say, τ does not generally enable the cancellation of the derivative of the mean curvature, hence $\mathcal{E}_W = O(w^3)$.

We have now explicitly constructed a family of solutions whose associated energies are of the same order as the equilibrium energy in the presence of constraints, obtained by minimizing the reduced energy (33). It can be shown (see Appendix C) that regardless of the metric φ, and in the absence of constraints, the minimal energy is always obtained for $\tau = 0$ (see, e.g., Fig. 8).

C. The $\beta \to 0$ singular limit

For every metric for which $\beta = 2\kappa_g - k'(0) = 0$ the optimal $\mathcal{E}_W = O(w^5)$ solution is continuously symmetry (the second fundamental form is independent of x_2). In view of the results of the previous section, the midline of the optimal solution has zero torsion, hence it lies in a plane. However, considering the $\beta \to 0$ limit, we encounter solutions that not only do not lie on a plane but even become exceedingly convoluted as $\beta \to 0$.

This seeming contradiction is due to the presence of two limiting processes; the limit $L \to \infty$ cannot be interchanged with the limit $\beta \to 0$. For $\beta \neq 0$ the solutions have period $2\pi/\beta$, which implies that every strip of finite length is short for sufficiently small β. Our above solution for strips of finite length yield that as $\beta \to 0$ the optimal phase is obtained at $\theta \to \pi/4$, placing the finite strip in a region in which the midcurve is almost planar.

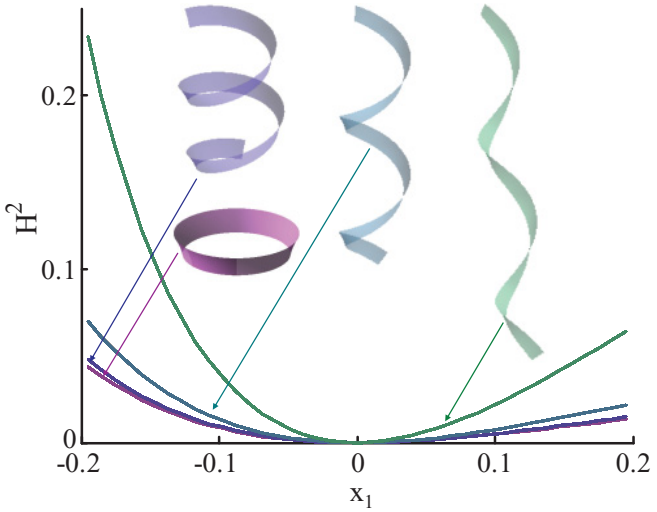

FIG. 8. (Color online) Translationally invariant configurations of various pitch. H^2 as function of x_1 for four different embeddings of the pseudospherical metric (14) ($K = -1$ everywhere) for the parameters $\kappa_g = 0.4$, $w = 0.4$, and $L = 4\pi$. In all cases $H = 0$ along the midcurve and the configurations differ by the value of τ. The inset shows the solutions to $\tau = 0, -7/25, -3/5, -15/17$ (left-to-right) next to their corresponding curves.

Example. For the pseudospherical metric (14), the $O(w^5)$ contribution to the Willmore energy is

$$w^5 \frac{9}{2^{10}5} \int_{-L/2}^{L/2} \frac{\left(1+r_0^2\right)^2}{r_0^2} dx_2 = -\frac{w^5}{\beta} \frac{9}{2^8 5} \cot(\beta x_2 + 2\theta) \Big|_{-L/2}^{L/2},$$

which is minimized at the phase value of $\theta = \pi/4$ for all choice of β. Fig. 9 illustrates how this choice of phase places the finite strip in a region that resembles the $\beta = 0$ continuously symmetric solutions.

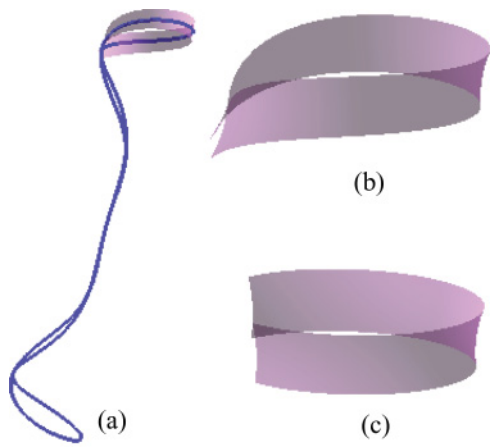

FIG. 9. (Color online) The $\beta = 0$ limit for finite strips. As $\beta \to 0$ we expect the solutions obtained to converge to the $\beta = 0$ solution. Optimizing for the location within the midcurve of a $\beta \neq 0$ solution (the phase θ) yields a strip segment very similar to that obtained for $\beta = 0$. (a) One period (of length $\lambda = 2\pi/\beta$) of the midcurve for a strip with metric (14) and $\kappa_g = 0.1$ along with a strip segment of length $\lambda/10$. Optimization with respect to the phase finds which segment along the period has the smallest Willmore energy. (b) The strip segment enlarged. (c) The $\tau = 0$ continuously symmetric strip for the same values of length and width.

VII. DISCUSSION

In this paper we presented a general approach to a class of elastic problems that arise in shape selection of naturally forming thin and elongated strips. Specifically, we consider strips that have a plate-like structure (i.e., no structural variation across the thin dimension), whose intrinsic two-dimensional geometry is hyperbolic. The first step is the reduction of the three-dimensional elastic problem into the purely geometric problem of isometrically embedding a surface with given metric in three-dimensional space. This reduction is justified in the limit of vanishing thickness [10]. In this limit the equilibrium configuration corresponds to the bending-minimizing isometry. In a second step, we take advantage of (i) the hyperbolic nature of the embedding problem which enables the determination of the surface by solving an "evolution equation" so that embedding a single curve determines the shape of the whole surface and (ii) the existence of a second small scale, the width of the strip. Combining these two properties we construct approximate minimizers of the bending energy in which the mean curvature and its normal derivative vanish along the midcurve of the strip.

While embedding problems and minimal surfaces are classical fields of study in geometry, the present work offers a different perspective on both problems, interconnecting them. Our task consists of minimizing the Willmore functional given a metric (rather than given a topology [29]). This leads us to consider minimal embeddings of certain metrics. In this context we recover the continuous family of minimal isometric of the catenoidal metric ([22], p. 121). For general metrics satisfying the Ricci condition minimal embeddings of infinitely long strips are unique.

The reduced one-dimensional problem obtained in the thin-and-narrow limit yields an elastic energy that only depends on the embedding of a curve, that is, on curvature and torsion functions. In the context of rod theory, in the appropriate limit [19], the twist of the rod (the third degree of freedom in rod theory, e.g., [5], p. 61) is determined in our case by Gauss' equation. In particular, the various families of solutions obtained in this paper are a subclass of solutions arising in nonlinear rod theory under the choice of an appropriate energy density. As a consequence, some results from rod theory apply verbatim in our case. For example, the incorporation of periodic structural variations along the strip may induce chaotic configurations in certain cases [30].

The present work is formulated in a way that refers to the continuum limit of amorphous solids. However, we expect its applicability in a much larger context, for example, as discussed in the Introduction, in the conformation of some particular macromolecules. While in some cases it suffices to consider macromolecules as elastic rods [31], we show here how the introduction of nontrivial surface geometry may result in very intricate equilibrium configurations, even for very simple intrinsic geometries of unconstrained molecules.

ACKNOWLEDGMENTS

This work was supported by the United States–Israel Binational Foundation (Grant No. 2004037) and the Soft–Growth project of the ERC program for the European Union. This research was partially supported by the Israel Science Foundation. E.E. would like to thank M. Plummer for his help with *hyper-chem*.

APPENDIX A: EXISTENCE OF ALMOST-MINIMAL STRIPS

In Sec. V we constructed midcurves [the explicit formula is given by (B1)] of surfaces with prescribed (hyperbolic) metrics, subject to the condition that both the mean curvature and its first derivative vanish on the midcurve. In this Appendix we raise the question of whether such surfaces actually exist, namely does one have indeed the freedom to impose the shape of the midcurve. This question turns out to be highly nontrivial, for reasons we will explain, yet we argue that almost-minimal solutions can always be constructed, possibly requiring a slight modification of the procedure introduced in Sec. V.

By the fundamental theorem of surface geometry, given first and second fundamental forms that satisfy the GMPC equations (3), these forms are realizable by a surface (unique up to rigid transformations). For hyperbolic surfaces the GMPC equations may take the form (17). The question of existence then reduces to finding a solution to (17). The setting in Sec. V is such that initial data are prescribed along the $x_1 = 0$ parametric curve so that a solution has to be continued from this initial data curve on both sides.

Explicit solutions of the GMPC equations were found for metrics that admit minimal surfaces, but not for almost-minimal surfaces. The system (17) is hyperbolic, implying that solutions are propagating along characteristics, the latter coinciding with the asymptotic curves. To better understand the nature of the problem, we display in Fig. 10 the asymptotic curves that correspond to a minimal surface. The solid black line is the midcurve. From every point on the surface emerge two asymptotic curves (the two families of curves are represented by blue and red curves, respectively). The topological structure of the asymptotic curves determines the domain of influence of the initial data. At every point that can be connected to the initial data curve by a pair of characteristics, the solution is uniquely determined by the initial data. However, if a characteristic curve intersects the initial data curve twice, it may be prescribed with two contradicting initial values in which case no smooth solution exists. Such a situation arises when asymptotic curves are tangent to the initial data curve.

Examining Fig. 10 we see that it is possible to integrate the GMPC equation only on one side of the initial data curve unless the initial data satisfy precise compatibly conditions which cannot be expected in general. This apparent difficulty can be easily circumvented by prescribing the shape of the boundary curve $x_1 = -w/2$ rather than the midcurve. It is easy to see that imposing the vanishing of H and its first derivative on the boundary curve still guarantees a Willmore energy of order w^5, while resolving the problem of existence.

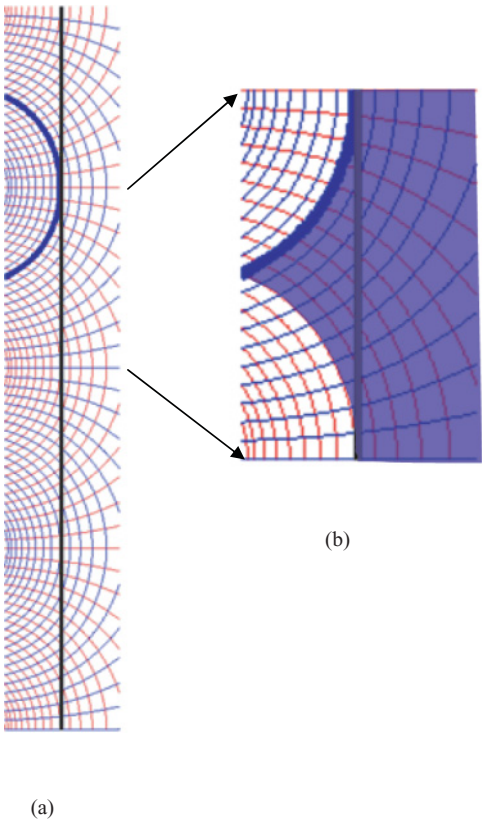

(a) (b)

FIG. 10. (Color online) Typical topology of the two families of asymptotic curves for a minimal surface of the type described in Sec. V. At every point two characteristic curves from distinct families intersect. (a) The straight bold (black) line is the midcurve along which initial data values are prescribed. One characteristic curve that is tangent to the midcurve is also bolded (blue). All characteristic curves from the same family which lay to the left of this curve do not intersect the midcurve, and therefore are uninfluenced by the initial data. Characteristic curves of the same family which lay to the right of this curve intersect the midcurve twice and may generate a conflict of initial data. (b) A blowup of a section of the strip. The shaded region marks the domain of influence of initial data given along the midcurve. Prescribing additional partial data along the bolded dashed (blue) line is needed in order to determine the solution uniquely in the unshaded region.

APPENDIX B: FORMULA FOR THE MIDCURVE OF AN ALMOST-MINIMAL STRIP

The tangent vector $\partial_2 \boldsymbol{f}$ along the midcurve of an almost-minimal strip is given by the explicit expression (24), with the integration constants **a**, **b**, and **c** given by (25). Integrating once more with respect to x_2 we obtain the midcurve

$$\begin{aligned}\boldsymbol{f}(0,x_2) &= \boldsymbol{f}(0,0) + \frac{\mathbf{a}}{\beta(\beta-\kappa_g)}\sin\beta x_2 \\ &\quad - \frac{\gamma\mathbf{b}}{\beta^2-\gamma^2}(\gamma\sin\beta x_2\cos\gamma x_2 - \beta\cos\beta x_2\sin\gamma x_2)\end{aligned}$$

$$
\begin{aligned}
&-\frac{\gamma \mathbf{c}}{\beta^2-\gamma^2}\,(\beta\cos\beta x_2\,\cos\gamma x_2+\gamma\sin\beta x_2\,\sin\gamma x_2)\\
&-\frac{(\beta-\kappa_g)\mathbf{b}}{\beta^2-\gamma^2}\,(\beta\sin\beta x_2\,\cos\gamma x_2-\gamma\cos\beta x_2\,\sin\gamma x_2)\\
&-\frac{(\beta-\kappa_g)\mathbf{c}}{\beta^2-\gamma^2}\,(\gamma\cos\beta x_2\,\cos\gamma x_2+\beta\sin\beta x_2\,\sin\gamma x_2).
\end{aligned}
\tag{B1}
$$

APPENDIX C: TRANSLATIONALLY INVARIANT SOLUTIONS

In this Appendix we focus our attention on configurations that are translationally invariant, that is, both fundamental forms do not depend on x_2, and find the energy minimizer within this family of configurations. This is an ansatz that restricts the set of admissible functions in the variational problem. Note also that this symmetry assumption ignores end effects, so we are considering in practice an infinite strip, and energies will be computed per-unit-length (of the midcurve $x_1 = 0$). The fact that the shape of the strip is invariant under shifts in x_2 has two immediate consequences.

(1) Every two constant-x_2 curves differ by a rigid motion.
(2) Every constant-x_1 curve is a helix.

The first consequence is due to the fact that the Weingarten equations do not depend explicitly on x_2. The second consequence follows from the fact that the curvature and torsion (as a curve in $\mathbb{R}^3$) of constant-x_1 curves are determined by the first and second fundamental forms, hence independent of x_2. Lancret's theorem states that a necessary and sufficient condition for a curve to be a helix is that the ratio of curvature to torsion be constant.

To fully characterize the midcurve it remains to determine its curvature and torsion which can be obtained through the Weingarten equations

$$
\tau = b_{12} \quad \text{and} \quad \kappa = \sqrt{\kappa_g^2+\kappa_n^2} = \sqrt{\varphi'^2+b_{22}^2}, \tag{C1}
$$

where κ_n is the normal curvature of the midcurve and all terms on the right-hand sides are estimated at $x_1 = 0$. Thus we may write the midcurve in explicit form

$$
\boldsymbol{f}(0,x_2) = \frac{1}{\mu}[\sin(\psi)\,\cos(\mu\,x_2),\,\sin(\psi)\,\sin(\mu\,x_2),\,\cos(\psi)\mu\,x_2],
$$

where we have defined μ and ψ via $\mu^2 = \kappa^2+\tau^2$ and $\tau = \mu\cos(\psi)$. We now consider again the GMPC equations in Riemann invariant form (17) imposing the translational symmetry condition. Since the variables r and s are expressible in terms of the first and second fundamental forms, they are independent of x_2 in which case (17) reduces to a pair of ordinary differential equations for $r = r(x_1)$ and $s = s(x_1)$,

$$
\begin{aligned}
r' &= A_1 r + A_2 s + A_5 r^2 s,\\
s' &= A_1 s + A_2 r + A_5 s^2 r,
\end{aligned}
\tag{C2}
$$

where the coefficients A_i are given by (18). We solve this system on the interval $[-w/2, w/2]$. Initial data r_0, s_0 are assumed to be prescribed on the midcurve. The system (C2) can be integrated analytically. Direct substitution shows that

$$
\begin{aligned}
\eta &= \varphi^2 k\,\frac{r+s}{r-s},\\
\xi &= \frac{k^2\varphi^2+(\varphi')^2}{4}+k^2\frac{1+\varphi^2 rs}{(r-s)^2}
\end{aligned}
\tag{C3}
$$

are constant under the dynamics (C2), that is, are independent of x_1. This implies at once that

$$
\eta = \frac{r_0+s_0}{r_0-s_0} \quad \text{and} \quad \xi = \frac{1+\kappa_g^2}{4}+\frac{1+r_0 s_0}{(r_0-s_0)^2},
$$

where we have used our normalization whereby $\varphi(0) = k(0) = 1$ and the fact that $-\varphi'(0) = \kappa_g$. The initial data r_0 and s_0 can be directly linked to the curvature and torsion of the midcurve by using relations (C1) and (7),

$$
r_0 = \frac{-\tau-1}{\kappa_n} \quad \text{and} \quad s_0 = \frac{-\tau+1}{\kappa_n}.
$$

Substituting into (C3) the constants of motion are given by

$$
\eta = \tau = \mu\cos(\psi) \qquad \text{and} \qquad \xi = \frac{\kappa^2+\tau^2}{4} = \frac{\mu^2}{4}.
$$

Thus, the solution $r(x_1)$ and $s(x_1)$ of (C2) is given by the implicit relations

$$
\begin{aligned}
\mu\cos(\psi) &= \varphi^2 k\,\frac{r+s}{r-s},\\
\mu^2 &= k^2\varphi^2+(\varphi')^2+4k^2\frac{1+\varphi^2 rs}{(r-s)^2}.
\end{aligned}
$$

Straightforward algebraic manipulations lead to

$$
\begin{aligned}
(r-s)^2 &= \frac{4k^2\varphi^2}{\mu^2\varphi^2-\mu^2\cos^2(\psi)-\varphi^2(\varphi')^2},\\
rs &= \frac{\tau^2/\varphi^2-k^2\varphi^2}{\mu^2\varphi^2-\mu^2\cos^2(\psi)-\varphi^2(\varphi')^2},\\
(r+s)^2 &= \frac{4\tau^2/\varphi^2}{\mu^2\varphi^2-\mu^2\cos^2(\psi)-\varphi^2(\varphi')^2},
\end{aligned}
\tag{C4}
$$

and the mean curvature is given by

$$
H = \frac{k(1+\varphi^2 rs)}{\varphi(r-s)} = \frac{\mu^2-(\varphi')^2-\varphi^2k^2}{2\sqrt{\mu^2\varphi^2-\mu^2\cos(\psi)^2-\varphi^2(\varphi')^2}}. \tag{C5}
$$

We have obtained an explicit expression for the mean curvature as function of x_1 in terms of the "initial data parameters" κ and τ (or equivalently, μ and ψ) and the metric function $\varphi(x_1)$. A first observation is that the solution has a "finite horizon"; the domain of integration is limited by the requirement that the denominators in (C4) remain positive. For fixed κ and τ the width of the strip w has to be small enough such that

$$
\kappa^2\varphi^2+\tau^2(\varphi^2-1)-\varphi^2(\varphi')^2 > 0,
$$

where φ and φ' are evaluated at $\pm w/2$. Alternatively, fixing w, the range of admissible κ and τ lies outside an ellipse. Referring to the family of immersions introduced in [26], characterized by a small parameter which corresponds to how tight the initial curve is wound up, it is no surprise that by setting κ high enough we may avoid the finite horizon for a given width. Such tightly wound configurations, however, have a high cost in terms of bending. Limiting our attention to low-energy configurations, we use the above inequality as a restriction on the width w. Setting κ^2 and τ^2 to their lowest possible values ($\kappa_n^2 + \kappa_g^2$ and 0, respectively) and approximating $\varphi' \approx \kappa_g + \kappa^2 x_1$ we obtain for almost minimal strips

$$\kappa_g w + \tfrac{1}{4}\kappa^2 w^2 < 1,$$

implying that the width must be smaller than each of the two local geometric length scales of the problem κ_g^{-1} and κ^{-1}, which, no surprise, coincides with the previous definition of parameter regime. A second observation is that the mean curvature (C5) is minimized at $\psi = \pi/2$ regardless of μ and φ. This corresponds to zero torsion, that is, planar midcurves.

[1] E. Sharon, M. Marder, and H. L. Swinney, Am. Sci. **92**, 254 (2004).
[2] R. Vandivier and A. Goriely, Europhys. Lett. **84**, 58004 (2008).
[3] C.-C. Wang, Arch. Ration. Mech. Anal. **23**, 1 (1966).
[4] E. Kroner, The physics of defects, in *Les Houches Summer School Proceedings*, edited by R. Balian, M. Kleman, and J.-P. Poirier (North-Holland, Amsterdam, 1981).
[5] A. E. H. Love, *A Treatise on the Mathematical Theory of Elasticity*, 4th ed. (Cambridge University Press, Cambridge, 1927).
[6] E. Efrati, E. Sharon, and R. Kupferman, J. Mech. Phys. Solids **57**, 762 (2009).
[7] Y. Klein, E. Efrati, and E. Sharon, Science **315**, 1116 (2007).
[8] E. Sharon and E. Efrati, Soft Matter **6**, 5693 (2010).
[9] E. Efrati, E. Sharon, and R. Kupferman, Phys. Rev. E **80**, 016602 (2009).
[10] M. Lewicka and M. R. Pakzad, ESAIM: Control, Optimisation and Calculus of Variations (2011).
[11] The illustrations in Fig. 2 rendered through *Hyper-chem* are not intended to describe real molecules in a natural environment. The carbon rings are not aromatic and no hydrogens were added to boundary atoms. Equilibrium configurations were obtained by geometric optimization (zero temperature limit) in vacua. To ensure stability of the configurations, molecular dynamics at room temperatures were invoked and followed by geometric optimization steps until a unique geometric optimization solution was reproducibly obtained.
[12] H. Liang and L. Mahadevan, Proc. Natl. Acad. Sci. USA **106**, 22049 (2009).
[13] M. A. R. Koehl, W. K. Silk, H. Liang, and L. Mahadevan, Integrative Comparative Biol. **48**, 834 (2008).
[14] E. D. Sone, E. R. Zubarev, and S. I. Stupp, Ang. Chem. Int. Ed. **41**, 1705 (2002).
[15] M. Sadowsky, Proc. 3rd Int. Congr. Appl. Mech. **2**, 444 (1931).
[16] E. H. Mansfield, Q. J. Mech. Appl. Math. **8**, 338 (1955).
[17] E. L. Starostin and G. H. M. van der Heijden, Nat. Mater. **6**, 563 (2007).
[18] M. Marder and N. Papanicolaou, J. Stat. Phys. **125**, 1069 (2006).
[19] L. Mahadevan and J. B. Keller, Proc. R. Soc. **440**, 149 (1993).
[20] C.-C. Wang, Arch. Ration. Mech. Anal. **27**, 33 (1967).
[21] E. Efrati, E. Sharon, and R. Kupferman (to be published).
[22] D. J. Struik, *Lectures on Classical Differential Geometry*, 2nd ed. (Dover, New York, 1961).
[23] R. Kupferman and Y. Shamai (submitted).
[24] T. J. Willmore, *An Introduction to Differential Geometry* (Clarendon, New York, 1959).
[25] B. L. Rozhdestvenskii, Doklady Akademii Nauk (SSSR), **143**, 50 (1962).
[26] E. G. Poznyak and E. V. Shikin, Amer. Math. Soc. Transl. Ser 2, **176**, 151 (1996).
[27] L. C. Evans, *Partial Differential Equations* (American Mathematical Society, Providence, MA, 1998).
[28] S.-S. Chern and R. Osserman, *Geometry Symposium*, Volume 894 of *Lecture Notes in Mathematics*, edited by E. Looijenga, D. Siersma, and F. Takens (Springer, New York, 1981), pp. 49–90.
[29] T. J. Willmore, in *Geometry and Topology of Submanifolds* (World Scientific, Leuven, 1992), Vol. IV, pp. 11–16.
[30] M. A. Davies and F. C. Moon, Chaos **3**, 93 (1993).
[31] I. Klapper, J. Comput. Phys. **125**, 325 (1996).